Noninvasive MRI evaluation of cerebral blood flow in cerebrovascular disease

J.A. Detre, MD; D.C. Alsop, PhD; L.R. Vives, MD; L. Maccotta; J.W. Teener, MD; and E.C. Raps, MD

Article abstract—Previous studies have demonstrated that cerebral blood flow (CBF) can be assessed noninvasively by MRI using magnetic labeling of arterial water as a diffusible flow tracer. The purpose of this study was to assess the quality of CBF images obtained from patients with cerebrovascular disease using this method, and to begin to evaluate the potential clinical role for this technique. We recruited 14 patients who presented with stroke, TIA, or severe carotid stenosis and were likely to have altered CBF based on clinical assessment. In many of these patients, CBF imaging disclosed both focal and hemispheric hypoperfusion, either in vascular territories or in watershed regions. In 11 patients with significant proximal arterial stenosis, hemispheric CBF abnormalities localized to the side of most significant stenosis for the anterior circulation distribution. In several patients watershed hypoperfusion was even more pronounced. Our results suggest that good-quality MR CBF images can be obtained reliably from patients with cerebrovascular disease. CBF imaging can be combined with standard structural imaging within a single MRI examination, and provides clinically meaningful information. The capability of measuring CBF easily provides a potentially useful tool for clinical assessment and further investigation of stroke pathophysiology.

NEUROLOGY 1998;50:633–641

Although MRI is generally considered to be a technique for imaging brain structure, a variety of MRI methods are sensitive to the effects of cerebral blood flow (CBF).[1-3] Previous studies in both animals and in humans have demonstrated that MR images of CBF can be obtained noninvasively and quantitatively using magnetic spin labeling of arterial water as a diffusible flow tracer.[3-9] In this approach arterial water is labeled magnetically proximal to the brain using spatially selective radio frequency (RF) pulses. The method is entirely noninvasive and requires neither catheterization of vessels nor exogenous tracers. The effects of arterial spin labeling (ASL) on distal images can be quantified in terms of tissue blood flow because the regional changes in signal intensity are determined by an interaction between blood flow, which delivers labeled spins to the tissue, and T_1 relaxation, which causes the label to decay. CBF can be calculated based on a knowledge of the signal change with and without ASL and T_1, which are all measurable parameters.[2] We have recently improved the quality of CBF images obtained from human subjects using this technique by reducing sensitivity to transit effects[4] and extending the protocol to multislice imaging.[10] CBF data obtained in this way may potentially contribute to the management of patients with cerebrovascular disease and could be acquired as part of a standard MRI protocol.

The purpose of this study was to assess the quality of CBF images obtained from patients with cerebrovascular disease using the ASL method and also to begin to evaluate the potential clinical role for this technique. A related single-slice ASL technique was recently validated in patients with stroke[11] and was shown to provide a comparable CBF assessment to contrast-based studies. We recruited patients who presented with stroke, TIA, or severe carotid stenosis and were likely to have altered regional CBF, either focally or globally, based on clinical assessment. MR CBF images were obtained using the continuous arterial spin labeling (CASL) method.[4,6,7] Although the CASL method can be made relatively insensitive to arterial blood velocity, this approach has not been widely tested in patients with cerebrovascular disease and proximal arterial stenoses. Both the presence of stenoses and the resulting prolonged transit times are potential sources of error or artifact in CBF imaging by this method.

Hypoperfusion is the proximate cause of all ischemic stroke, yet the extent of its role as a primary etiology of stroke remains uncertain.[12] Several studies have measured regional brain perfusion in patients with stroke and TIA in an effort to elucidate the contribution of primary hypoperfusion in vascular territories to stroke incidence. In these studies, regional measurements of cerebral perfusion or perfusion reserve were correlated with the presence of extracranial stenoses of the carotid arteries.[13-16] Most but not all studies failed to implicate primary hypo-

From the Departments of Neurology (Drs. Detre, Vives, Maccotta, Teener, and Raps) and Radiology (Drs. Detre and Alsop), University of Pennsylvania, Philadelphia, PA.

Supported by NS01668 (JAD), a grant from the Whitaker Foundation (DCA), and the University of Pennsylvania Stroke and Neuro-Intensive Care Research Fund.

Received February 14, 1997. Accepted in final form April 5, 1997.

Address correspondence and reprint requests to Dr. John A. Detre, Department of Neurology, University of Pennsylvania, 3400 Spruce Street, Philadelphia, PA 19104.

perfusion clearly as a cause of large-vessel stroke, however hypoperfusion was found to be predictive of recurrent stroke.[17-19] While so-called border zone or watershed infarctions have clearly been associated with reduced systemic perfusion, the contribution of this mechanism to overall stroke incidence is thought to be low. Interestingly, however, the presence of such strokes in patients presenting with stroke or TIA carries an extremely poor prognosis.[20] Recent evidence also suggests an etiologic role of primary hypoperfusion in white matter ischemic disease.[21-24] A secondary goal of this study was to determine whether resting hemispheric perfusion asymmetries could be detected in patients with cerebrovascular disease and whether any such asymmetries correlated with the clinical presentation.

Methods. *Patient recruitment.* Patients were recruited from the inpatient and outpatient services of the Division of Stroke and Neuro-Intensive Care, Department of Neurology, University of Pennsylvania Medical Center, and gave their informed consent to participate. Patients presenting with stroke, TIA, or other clinical evidence of abnormalities in cerebral perfusion were recruited. All patients had received a structural MRI and most patients had received a variety of other diagnostic tests including carotid ultrasound, transcranial Doppler, MR angiography, or conventional selective angiography. The results of these studies are briefly summarized in table 1. The majority of patients had significant unilateral or bilateral carotid stenosis. Patients with large cortical infarcts affecting the majority of any vascular distribution were excluded. None of the patients were studied using CASL within the first 24 hours of symptom onset.

Imaging methods. Imaging was performed on a 1.5-T SIGNA (GE Medical Systems, Milwaukee, WI) clinical scanner equipped with a prototype gradient system for echoplanar imaging. CBF imaging was typically combined with standard structural imaging including T1-weighted images obtained in sagittal and axial planes, and T2-weighted fast-spin echo images obtained in an axial plane. For measurements of CBF, gradient echo echoplanar images were obtained using a field of view of 24 cm along the frequency encoding direction and 15 cm for the phase direction, and an acquisition matrix of 64 × 40. An acquisition bandwidth of ±62.5 kHz allowed an effective TE of 22 msec and an image acquisition time of 45 msec. Multislice image acquisition was performed without pausing between slices so that eight slices could be acquired in less than 400 msec. A slice thickness of 6 or 8 mm was employed and an interslice gap of 2 mm was used to minimize any interference between slices. Slice locations were chosen to include supratentorial structures.

In CASL, the cephalad flow of arterial blood in the presence of an appropriate RF field and magnetic field gradient causes an adiabatic inversion of arterial water spins.[25] CASL was performed as previously reported for single-slice perfusion imaging,[4] except that an amplitude-modulated control pulse was used to allow the acquisition of more than one slice while controlling for magnetization transfer effects.[10] The use of continuous velocity-driven inversion maximizes the amount of spin labeling obtained, providing the greatest possible flow sensitivity for an ASL measurement. A TR of 4 sec, a labeling gradient of 0.25 g/cm, a labeling RF of 35 mg, temporal interleaving of labeled and control images, and a postlabeling delay of 1.5 sec were employed. The postlabeling delay dramatically reduces the sensitivity of the perfusion image to the transit time from the labeling plane and strongly attenuates the contribution of intraluminal arterial spins to the image intensity. The postlabeling delay also allows time for all of the labeled blood to enter the tissue before imaging so that saturation of tagged flowing spins by the multislice excitation pulses need not be considered. For the control image used to measure brain signal in the absence of arterial labeling, the labeling pulse was applied at the same location, but amplitude modulation of the RF was used to minimize its effectiveness for ASL.[26] Forty-five inversion/control pairs acquired in 6.5 min were used to measure the signal change with spin labeling.

In addition to the perfusion scan, multislice versions of the previously described echoplanar T1 mapping scans was performed.[4] The T1 maps are required for quantification of the perfusion images. It was necessary to leave the tagging gradient on during T1 mapping to measure accurately the T1 shortening effect of the off-resonance saturation. In all other ways the protocol was identical. The entire T1 mapping protocol required 3 min for all slices. A map of static magnetic field inhomogeneities was also acquired for subsequent distortion correction of echoplanar images (1 min).[27]

Data analysis. Raw image data were stored onto 4-mm tape during acquisition and processed off-line on SPARC workstations (Sun Microsystems, Mountain View, CA) using software written in Interactive Data Language 4.0 (Research Systems, Boulder, CO). Image reconstruction included automated phase correction and distortion correction for static magnetic field inhomogeneities.[28] A postprocessing algorithm to reduce motion artifact and physiologic noise was employed.[29] T1 maps with and without the spin tagging pulse were calculated as previously described.[4]

Perfusion was calculated from images acquired with and without arterial spin tagging, and from the T1 maps using a generalization of the formula

$$f = \exp\left(\frac{w}{T_{1app}}\right) \exp\left(\delta\left(\frac{1}{T_{1a}} - \frac{1}{T_{1app}}\right)\right) \frac{\lambda(M_b^{ctrl} - M_b^{tag})}{2\alpha M_b^{ctrl} T_{1app}}$$

where w is the post-tagging delay, δ is the transit time to the tissue, λ is the partition coefficient of water between blood and brain, α is the tagging efficiency, T_{1app} is the T1 of the tissue, and T_{1a} is the T1 of arterial blood. Because T_{1a} and T_{1app} of gray matter are very close, the calculated flow is insensitive to δ, the transit time, but we assume δ is 1.2 sec for the calculation. For the multislice perfusion imaging protocol, the tagging efficiency, α, was estimated at 0.67 based on simulations and experimental data.[10,30] A representative quantitative perfusion map obtained from a normal subject using this approach is shown in figure 1.

In regions of very low CBF with concomitant increased arterial transit times, bright intraluminal artifact was sometimes observed. An example of this from Patient 3 is shown in figure 2 (top). The presence of a bright intraluminal signal suggests that, despite a postlabeling delay of 1.5 sec, not all labeled arterial water has exchanged with tissue and some intraluminal label remains. The bright signal could possibly be mistaken for hyperperfusion and

Table 1 *Patient diagnostic tests*

Patient no.	Age (y)	Sex	Clinical history	Structural MRI	Carotid U/S and/or TCD	Angiography	Perfusion MRI global CBF (cc/100 g/min)	Perfusion MRI description
1	74	M	Recurrent R weakness +/− aphasia; prior L CVA	L≫R white matter ischemic Δ	nd/na	100% L ICA, 90% R ICA	Gray 21.2 White 6.4 Total 15.7	Global and L hypoperfusion; L posterior temporal focal hypoperfusion
2	39	F	Headache and seizures	Sigmoid/transverse sinus thrombosis; posterior temporal CVA	nd/na	nd/na	Gray 40.0 White 23.0 Total 33.1	Global and R hypoperfusion; L temporal/occipital focal hypoperfusion
3	45	M	Takayasu's arteritis, R hemiparesis and aphasia	L inferior frontal CVA	100% L CCA; 100% L ICA	L CCA, L ICA, and R VA occlusion	Gray 78.4 White 41.4 Total 67.2	Minimal asymmetry; L frontal hypoperfusion
4	75	M	R hemiparesis and aphasia	Ischemic Δ; L cerebellar CVA; L ICA stenosis	Normal carotids; ↑ L intracranial velocities	nd/na	Gray 33.3 White 20.8 Total 28.7	Moderate asymmetry; L temporal/occipital and L anterior temporal hypoperfusion
5	72	F	Orthostatic R hemiparesis and aphasia	R≫L white matter Δ; L striatocapsular and R PICA CVAs	Normal carotids; ↑ R intracranial velocities	L>R and posterior circulation intracranial stenoses	Gray 41.1 White 16.9 Total 33.8	L hypoperfusion, especially watershed; L temporal/occipital focal hypoperfusion
6	57	M	Prior posterior circulation infarct	L PICA CVA; L hemispheric ischemic Δ	≥70% L ICA; mild R ICA	100% L ICA	Gray 55.4 White 23.3 Total 41.3	Minimal asymmetry
7	79	F	Air embolus L ICA; R hemiparesis and aphasia	Extensive L hemispheric white matter Δ	Moderate R ICA stenosis; normal TCD	nd/na	Gray 60.8 White 40.6 Total 52.2	Normal
8	73	F	Orthostatic R hemiparesis and aphasia	L MCA and L posterior watershed CVAs; arterial stenoses	L ICA occlusion	nd/na	Gray 25.0 White 7.6 Total 20.0	Global and L hypoperfusion; L temporal/occipital focal hypoperfusion
9	26	F	Moyamoya disease with cognitive decline	Diffuse L>R watershed and cortical CVAs; ischemic Δ	Normal carotids; TCD multifocal stenoses	R≫L intracranial stenosis with collaterals	Gray 32.4 White 10.6 Total 26.5	Global hypoperfusion; L temporal/occipital and R temporal/parietal focal hypoperfusion
10	75	M	Orthostatic L hemiparesis and dysarthria	R frontoparietal and parietal/occipital CVAs, R lacunes	Severe R ICA stenosis; 50% L ICA	nd/na	Gray 59.65 White 27.8 Total 49.3	Minimal asymmetry; R parietal/occipital hypoperfusion
11	66	M	Progressive Δ MS; aphasia and L hemiparesis	Ischemic Δ in white matter and brainstem	nd/na	100% L ICA and R VA; critical R ICA	Gray 86.7* White 31.8* Total 63.8*	*Marked transit artifact affecting quantification; global hypoperfusion
12	76	M	L hemiparesis, dysarthria, and ataxia	White matter ischemic Δ; lacunes; R>L ICA stenosis	nd/na	nd/na	Gray 76.0 White 32.0 Total 59.5	Minimal asymmetry
13	74	F	Recurrent episodes of R hemiparesis and aphasia	L striatocapsular infarct	>80% R ICA; B intracranial stenoses	nd/na	Gray 57.6 White 27.7 Total 48.0	Minimal asymmetry
14	72	F	Asymptomatic bilateral carotid stenosis	B carotid stenosis; hypoplastic L P1 and PCOM	80–95% R ICA; 70–80% L ICA	nd/na	Gray 63.4 White 29.5 Total 49.3	Minimal asymmetry

U/S = ultrasound; TCD = transcranial Doppler; CBF = cerebral blood flow; M = male; F = female; L = left; R = right; B = bilateral; Δ = changes; CVA = cerebrovascular accident; ↑ = increased; nd/na = not done/not available; ICA = internal carotid artery; CCA = common carotid artery; VA = vertebral artery; PICA = posterior inferior cerebellar artery; MCA = middle cerebral artery; MS = mental status; P1 = P1 segment of the posterior cerebral artery; PCOM = posterior communicating artery.

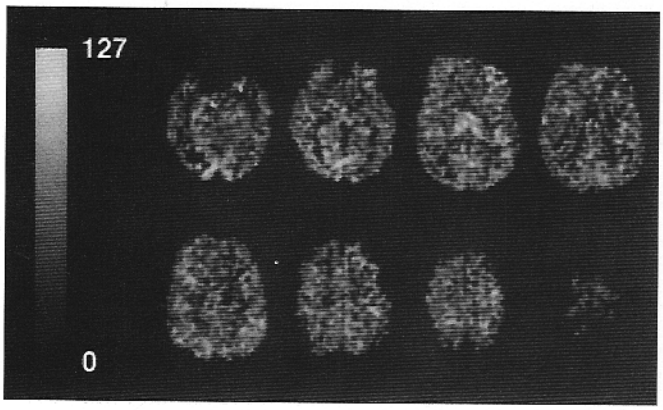

Figure 1. Multislice cerebral blood flow (CBF) imaging using the continuous arterial spin labeling method in a healthy 37-year-old male volunteer. Images were obtained in eight slices with a nominal pixel resolution of 3.75 × 3.75 × 8 mm. Grayscale shows CBF ranging from 0 to 127 mL/100 g/min. Increased CBF in cortical gyri and subcortical gray matter structures with reduced CBF in white matter is evident. CBF is symmetric bilaterally and without focal abnormalities. Some distortion due to magnetic field inhomogeneities is observed despite the correction procedure.

actually results in an underestimation of quantitative CBF in the distal field. Patient 11 had complete left carotid stenosis, critical right carotid stenosis, occlusion of the right vertebral artery, and markedly reduced flow through the left vertebral artery. In this patient, a diffuse bright signal was observed (figure 2, bottom), suggesting diffusely increased transit times of much greater than 1.5 sec. Away from the bright signal, cortical flow appears markedly reduced throughout. Quantification of CBF using regions of interest is therefore highly unreliable for Patient 11, as noted in table 1. Although this artifact precluded accurate quantification of CBF, it did suggest markedly abnormal hemodynamics. No other patient exhibited this degree of artifact. This source of artifact could be further reduced by increasing the postlabeling delay, at the expense of signal to noise. The postlabeling delay of 1.5 sec used in this study was a reasonable compromise between image quality and signal to noise for 1.5-T studies at our present resolution, although future work at higher magnetic field strengths or using other imaging schemes may allow a longer postlabeling delay to be used, resulting in improved image quality for patients with very long arterial transit times.

Multislice perfusion maps from patients were analyzed both by visual inspection and by region-of-interest analysis. The images were manually segmented into regions representing the anterior, middle, posterior, lenticulostriate, anterior watershed, and posterior watershed regions based on known anatomy. Only supratentorial structures were analyzed as slice coverage for this study limited data available from the cerebellum and brainstem. Within these regions, mean total CBF was determined as well as CBF in gray and white matter compartments, segmented based on T1 criteria. These data were further processed to determine an asymmetry ratio, $(L - R)/(L + R)$, for the anterior and posterior circulation distribution as well as for watershed distributions. The asymmetry ratio provides a measure of the lateralization of changes in CBF. For patients

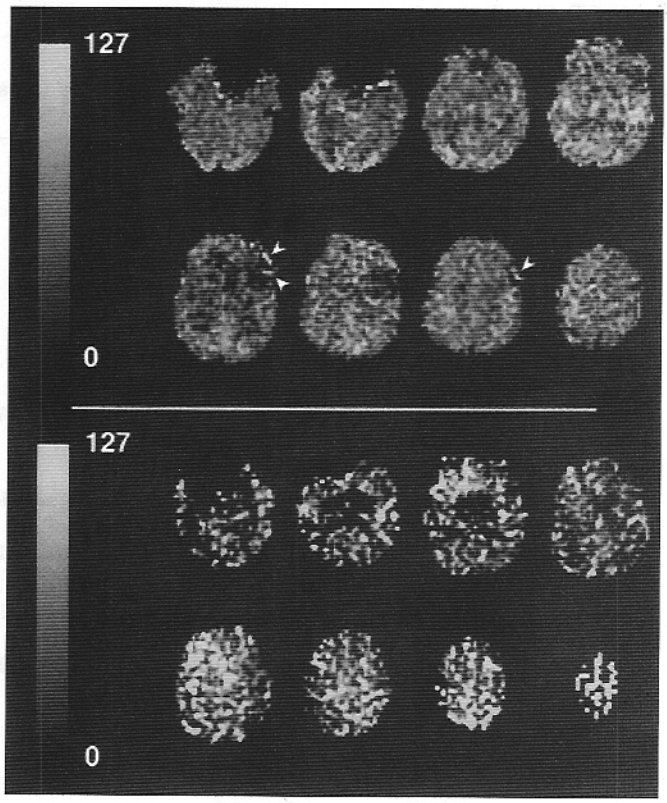

Figure 2. Intraluminal artifact in cerebral blood flow (CBF) images. Grayscale shows CBF ranging from 0 to 127 mL/100 g/min. (Top) CBF images from Patient 3. A focal region of hypoperfusion is evident in the left frontal lobe. Arrows indicate bright intraluminal artifact resulting from markedly delayed arterial transit times to the hypoperfused region, in this case likely due to pial collaterals. (Bottom) CBF images from Patient 11. Bright intraluminal artifact is observed diffusely, and degrades these images severely. Away from this artifact, cortical CBF is reduced.

with proximal arterial stenoses, the asymmetry ratios were compared with the lateralization of the most significant proximal stenosis, as determined clinically using conventional ultrasound, angiography, and MR angiography.

Results. Patient demographics, the results of independent clinical evaluation, and major findings with perfusion MRI are presented in table 1. All patients were able to complete the perfusion imaging protocol. Interpretable perfusion images were obtained in all patients, although the perfusion images from Patient 11 were highly degraded by transit artifact (see Methods). In many patients global and/or hemispheric abnormalities in perfusion were observed along with focal regions of hypoperfusion. Average CBF values across all patients for vascular regions of interest are listed in table 2. These values are in reasonable agreement with prior studies of perfusion in similar patients.[14,19,31,32] Due to partial volume effects, the white matter compartments actually contain a significant volume of gray matter, resulting in spuriously high flow values, although values are consistently much lower than gray matter flow values. Further, SDs are relatively higher in white matter than in gray matter because white matter CBF is

Table 2 *Average cerebral blood flow values for all patients*

Region of interest	Cerebral blood flow (cc/100 g/min)				
	Mean	Minimum	Maximum	SD	Mean voxels
Left PCA gray	56.5	20.5	91.6	21.9	360
Left PCA white	23.4	6.7	40.5	11.6	89
Left PCA total	47.1	16.5	78.7	18.0	450
Right PCA gray	57.7	25.3	89.5	19.1	329
Right PCA white	24.3	3.9	45.0	12.2	88
Right PCA total	47.7	20.6	77.2	16.2	418
Left MCA gray	50.2	13.7	84.0	21.3	1087
Left MCA white	24.6	3.9	44.7	12.4	416
Left MCA total	40.6	9.8	63.0	17.2	1504
Right MCA gray	52.0	24.9	93.5	21.0	1066
Right MCA white	23.1	8.2	38.6	9.5	431
Right MCA total	41.3	19.6	68.1	15.7	1497
Left LS gray	48.1	16.7	85.9	20.8	139
Left LS white	23.1	1.9	51.7	14.1	78
Left LS total	37.8	5.8	63.4	17.9	218
Right LS gray	51.9	20.2	86.9	20.3	52
Right LS white	30.9	3.1	65.3	16.4	14
Right LS total	44.3	12.9	77.7	19.6	66
Left ACA gray	46.8	13.4	81.0	21.1	213
Left ACA white	23.4	2.7	45.9	13.6	81
Left ACA total	38.7	8.7	71.0	19.2	294
Right ACA gray	51.6	26.2	101.4	21.8	230
Right ACA white	26.3	6.8	69.8	15.7	100
Right ACA total	42.3	19.5	89.3	18.9	330
Left posterior WS gray	47.0	3.4	78.4	23.4	128
Left posterior WS white	21.4	−0.8	37.8	13.5	55
Left posterior WS total	37.4	2.2	61.2	18.5	183
Right posterior WS gray	48.7	14.9	98.4	24.0	122
Right posterior WS white	18.1	3.2	41.4	11.3	59
Right posterior WS total	35.7	11.9	73.1	16.8	181
Left anterior WS gray	45.4	6.2	73.6	17.9	117
Left anterior WS white	18.4	1.0	44.4	12.7	65
Left anterior WS total	35.1	4.2	56.2	14.0	182
Right anterior WS gray	47.1	22.3	99.8	22.4	91
Right anterior WS white	24.6	8.0	51.7	13.4	68
Right anterior WS total	37.1	16.7	82.9	18.0	160
Focal region 1 gray	42.6	2.8	86.5	26.7	88
Focal region 1 white	17.2	−0.3	45.0	12.9	70
Focal region 1 total	28.0	1.1	58.0	16.3	159
Focal region 2 gray	30.6	7.7	46.0	15.1	124
Focal region 2 white	19.1	3.8	31.3	12.4	62
Focal region 2 total	24.5	6.8	36.0	11.8	186

PCA = posterior cerebral artery; MCA = middle cerebral artery; LS = lenticulostriate artery; ACA = anterior cerebral artery; WS = watershed zone.

Table 3 *Comparison of hemispheric asymmetries by clinical evaluation and perfusion imaging*

Patient no.	Clinical laterality[2]	Gray matter asymmetry ratios[1]		
		Anterior circulation	Posterior circulation	Watershed region
1	Left > right	−0.63	−0.21	−0.83
3	Left	−0.10	0.02	−0.30
4	Left	−0.17	−0.27	0.11
5	Left > right	−0.09	0.05	−0.25
6	Left > right	−0.02	−0.02	−0.01
8	Left > right	−0.15	−0.02	−0.46
9	Left > right	−0.04	−0.26	0.08
10	Right	0.11	0.17	0.22
11	Right > left	−0.13	0.12	−0.47
12	Right	0.00	0.03	0.19
13	Left	−0.04	−0.14	0.00
14	Right > left	0.04	−0.04	0.20

[1] Dimensionless, calculated as [(left − right)/(left + right)].
[2] Based on results of carotid ultrasound, transcranial Doppler, arteriography, and magnetic resonance angiography.

lower, and thus more difficult to measure. In consideration of this, a subsequent analysis of asymmetry ratios for the purpose of comparison with clinical laterality in patients with proximal arterial stenoses was carried out using only CBF values from the gray matter compartment.

Of the 14 patients studied, 12 patients presented with significant proximal arterial stenoses of the anterior circulation. Patient 11 was excluded because extensive intraluminal artifact precluded a region-of-interest analysis. In the remaining 11 patients, asymmetry ratios were calculated for the anterior circulation, posterior circulation, and watershed regions, and the results were compared with the laterality of the significant arterial stenoses determined by routine clinical investigation. These results are summarized in table 3. Of these 11 patients, all but one, Patient 6, showed asymmetry ratios in at least one vascular distribution greater than an arbitrary threshold of 0.1, equivalent to approximately a 20% difference in hemispheric values. Of note, Patient 6 had sustained a cerebellar stroke, but was asymptomatic with regard to supratentorial structures despite complete carotid stenosis by angiography. In the remainder of patients, for the anterior circulation there was complete agreement between the laterality of the clinically identified predominant stenosis and the laterality of perfusion deficit. In seven of these patients, greater asymmetries were observed in watershed regions than in the anterior circulation, although in three patients the laterality of border zone asymmetry differed from the clinically determined laterality.

In several patients with reduced blood flow and hemispheric asymmetries, T2-weighted structural imaging also revealed asymmetries in white matter signal intensities. An example of this from Patient 1 is shown in figure 3. This patient had bilateral intracranial carotid stenosis and recurrent episodes of right hemiparesis, frequently associated with aphasia. Perfusion imaging disclosed global but also quite asymmetric reduced flow (see figure 3, top). T2-weighted images showed marked asymmetry in white matter lesions, which were much more evident in the left hemisphere (see figure 3, bottom).

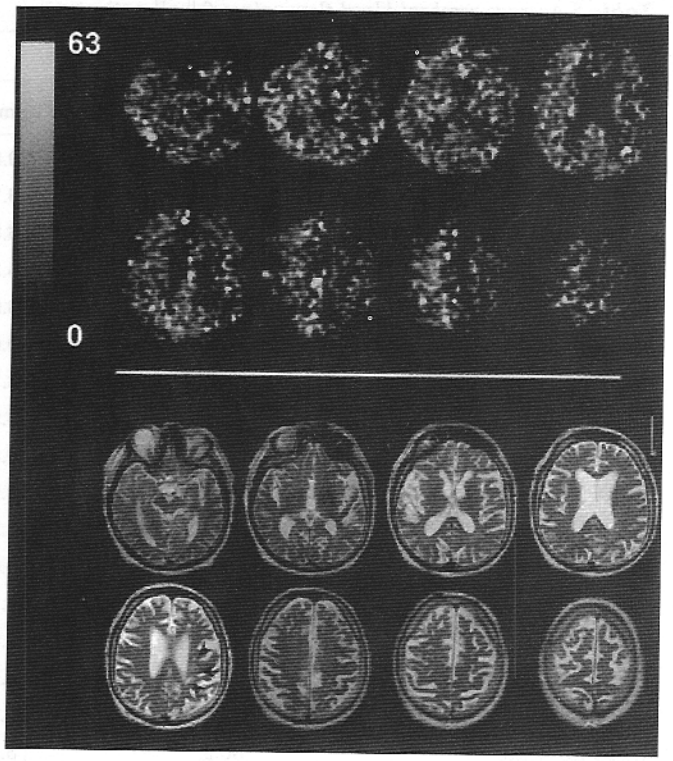

Figure 3. Cerebral blood flow (CBF) images and T2-weighted images from Patient 1. (Top) CBF is decreased both globally and asymmetrically, with markedly decreased flow in the left hemisphere, most notable in watershed regions. Grayscale shows CBF ranging from 0 to 63 mL/100 g/min. (Bottom) T2-weighted images show bilateral periventricular white matter changes. Arrows indicate asymmetric ischemic changes in the subcortical white matter that are likely the sequelae of hypoperfusion.

Patient 10 presented with right carotid stenosis and left hand weakness, and was found to have a right parietal subcortical infarct extending toward the motor cortex (figure 4, top). Perfusion imaging disclosed a much larger region of hypoperfusion affecting the right posterior watershed region (see figure 4, bottom). In contrast, an opposite disparity between results of perfusion imaging and structural imaging was observed in Patient 7 and is shown in figure 5. This patient had received an accidental air embolus during selective angiography of the left carotid artery and developed a right hemiparesis and aphasia. T2-weighted images showed extensive subcortical changes in the left hemisphere (see figure 5, top), while perfusion imaging showed normal CBF bilaterally (see figure 5 bottom). This patient subsequently recovered normal neurologic function, and follow-up T2-weighted MRI showed dramatic resolution of the subcortical signal changes. Patient 2 manifested decreased perfusion due to venous stasis (see table 1).

Discussion. The primary purpose of this study was to assess the feasibility of mapping CBF in patients with cerebrovascular disease using MRI with the CASL technique. The imaging protocol was well

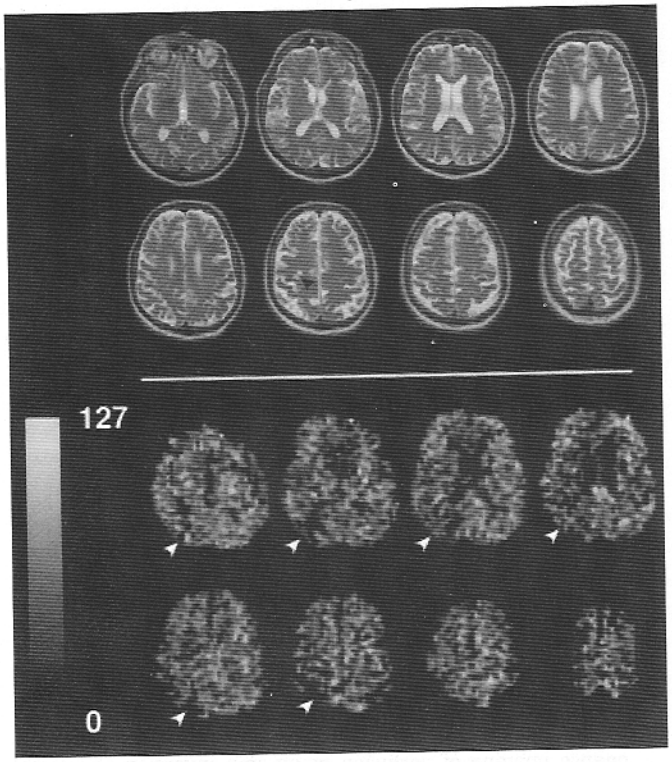

Figure 4. Cerebral blood flow (CBF) images and T2-weighted images from Patient 10. (Top) T2-weighted images show subcortical ischemic changes in the right parietal lobe abutting the motor cortex (black arrow). *(Bottom) CBF images show more widespread hypoperfusion in the right posterior watershed distribution* (white arrows). *Grayscale shows CBF ranging from 0 to 127 mL/100 g/min.*

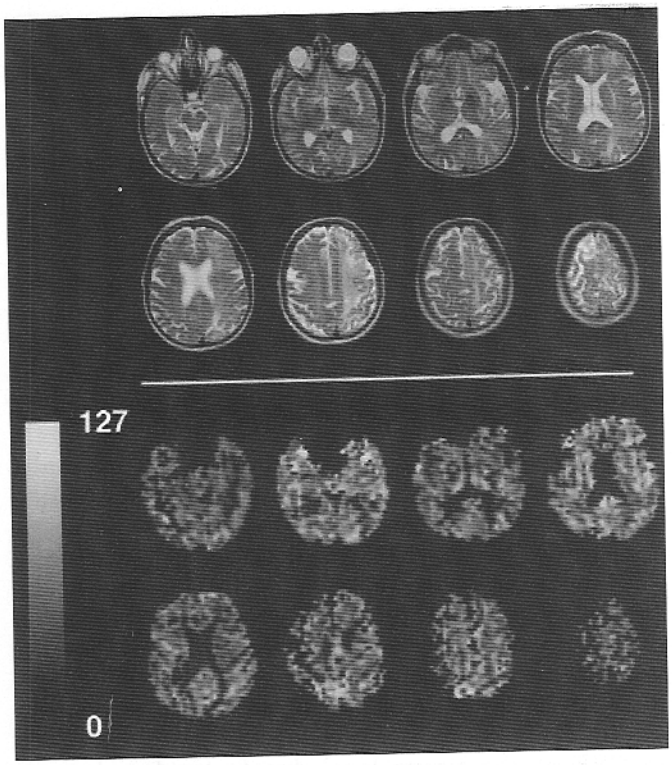

Figure 5. Cerebral blood flow (CBF) images and T2-weighted images from Patient 7. (Top) T2-weighted images show widespread signal hyperintensities throughout the white matter on the left. (Bottom) CBF images do not reveal any corresponding hemispheric changes, and CBF values are in a normal range. Grayscale shows CBF ranging from 0 to 127 mL/100 g/min.

tolerated and could be combined easily with a routine cerebrovascular MRI protocol. CASL theoretically affords the maximum sensitivity in ASL perfusion techniques as compared with pulsed labeling techniques,[3,11] and has been implemented successfully as a multislice protocol. Despite the presence of significant arterial occlusive disease in most of the patients studied, CASL was sufficient to produce good perfusion contrast. Further, degradation of CBF images due to increased transit times, manifested as bright focal artifact in perfusion images, was not severe or limiting except in Patient 11, who had truly end-stage cerebrovascular disease. Reduced CBF—either globally, hemispherically, or focally—was observed in nearly all of the patients. Consistent with this, several patients experienced orthostatic exacerbation of their neurologic deficits or recurrent TIAs in a single vascular distribution. One patient was symptomatic from a venous thrombosis, which can affect CBF as a result of venous stasis. The finding of reduced CBF in this patient suggests a role of CBF imaging in the assessment and management of raised intracranial pressure.

Anterior and posterior cortical watershed infarcts represent the most widely recognized structural correlate of hemodynamic infarction. Previous studies have suggested that white matter infarcts at the terminal distributions of vessels may be a more common consequence of hypoperfusion.[21,23] In this limited study we observed both cortical and subcortical infarcts in patients with reduced cerebral CBF. As has been noted previously,[23] the zone of reduced CBF was typically much greater than the region of actual infarction as assessed by T2-weighted imaging. Our observation of CBF abnormalities in cortical watershed territories, even in the absence of overt infarction, is consistent with the concept that these territories are uniquely sensitive to hemodynamic effects.

Previous studies that have assessed hemodynamic reserve in watershed territories in patients with carotid occlusive disease have conflicted with regard to the sensitivity of such measurements.[13,14] We attribute the high rate of watershed hypoperfusion in our study to patient selection, which specifically targeted patients with hemodynamic compromise. Because autoregulatory mechanisms in the cerebral vasculature can maintain CBF through vasodilation, it has been suggested that CBF alone is an inadequate measure of hemodynamic compromise.[12] Greater sensitivity is obtained by using measures of hemodynamic reserve by measuring cerebral blood volume (CBV) separately or by measuring the response to a pharmacologic vasodilator such as CO_2 or acetazolamide. Such agents could be administered

easily during MRI measurement of CBF. Compensated hemodynamic abnormalities are also manifested as an increase in mean transit time (MTT), which is mathematically equivalent to CBV/CBF.[13] CBF images obtained with ASL are sensitive to transit effects,[4,33] and by varying labeling parameters parametrically, the arterial portion of the transit delay can be estimated.[4,34] While the arterial transit time is not identical to MTT, it is clearly sensitive to hemodynamic compromise, as shown in figure 2. In this study we used a postlabeling delay to reduce this effect. It would also be possible to measure the arterial transit time using ASL, at the expense of a longer acquisition.

Although this study was not designed specifically to test the sensitivity or specificity of MRI for detecting CBF abnormalities distal to arterial stenoses, analysis of hemispheric asymmetries in measured CBF did show concordance with the findings of angiographic and ultrasonic studies. In the few patients in whom CBF asymmetries differed from the laterality of proximal stenosis, the disagreement between CBF and vascular evaluation may have represented real differences in the cumulative reduction in CBF at the tissue level due to tandem lesions, rather than an error in either measurement. The ability to assess the actual delivery of CBF at the tissue level represents the most significant benefit of adding a CBF imaging study to the evaluation of cerebrovascular disease.

Additional applications of CBF imaging to stoke triage and the clinical investigation of cerebrovascular disease can be envisioned. The presence of hyperperfusion in the distribution of an acute deficit suggests a favorable prognosis,[35] likely due to spontaneous early recanalization,[36] and may represent a contraindication to thrombolytic therapy. In contrast, very low regional CBF has been associated with poor outcome from thrombolytic therapy,[37] and may suggest a poor risk/benefit ratio for this therapy in selected patients. While a single CBF measurement alone is unlikely to determine the potential for reversibility in acute stroke, CBF measurements may be used to define the territory at risk or "ischemic penumbra"[38-40] and therefore may be useful in the assessment of stroke therapies. Such data would complement results of diffusion imaging, which delineates regions of ongoing cytotoxic injury in acute stroke.[41-43]

In summary, we have demonstrated that multislice CBF imaging using MRI with CASL can be conducted successfully in patients with cerebrovascular disease. Data acquisition time for this study was approximately 10 min, allowing it to be combined with standard structural imaging within a single MRI examination. At least in selected patients with cerebrovascular disease, CBF imaging using CASL can disclose both focal and hemispheric hypoperfusion, either in vascular territories or in watershed regions. The capability of measuring and quantitating tissue perfusion easily in such patients provides a useful tool for the clinical assessment and further investigation of stroke pathophysiology.

Acknowledgments

We gratefully acknowledge the technical assistance of Norman Butler, Tanya Kurtz, and Doris Cain-Edwards. Jeannie Dora and Jeannie Luciano provided assistance with clinical coordination.

References

1. Rosen BR, Belliveau JW, Chien D. Perfusion imaging by nuclear magnetic resonance. Magn Reson Q 1989;5:263–281.
2. Detre JA, Leigh JS, Williams DS, Koretsky AP. Perfusion imaging. Magn Reson Med 1992;23:37–45.
3. Edelman RR, Siewert B, Darby DG, et al. Qualitative mapping of cerebral blood flow and functional localization with echo-planar MR imaging and signal targeting with alternating radio frequency. Radiology 1994;192:513–520.
4. Alsop DC, Detre JA. Reduced transit-time sensitivity in noninvasive magnetic resonance imaging of human cerebral blood flow. J Cereb Blood Flow Metab 1996;16:1236–1249.
5. Detre JA, Zhang W, Roberts DA, et al. Tissue specific perfusion imaging using arterial spin labeling. NMR Biomed 1994; 7:75–82.
6. Roberts DA, Detre JA, Bolinger L, Insko EK, Leigh JS Jr. Quantitative magnetic resonance imaging of human brain perfusion at 1.5 T using steady-state inversion of arterial water. Proc Natl Acad Sci USA 1994;91:33–37.
7. Williams DS, Detre JA, Leigh JS, Koretsky AP. Magnetic resonance imaging of perfusion using spin inversion of arterial water. Proc Natl Acad Sci USA 1992;89:212–216.
8. Kwong KK, Chesler DA, Weisskoff RM, et al. MR perfusion studies with T1-weighted echo planar imaging. Magn Reson Med 1995;34:878–887.
9. Kim SG. Quantification of relative cerebral blood flow change by flow-sensitive alternating inversion recovery (FAIR) technique: application to functional mapping. Magn Reson Med 1995;34:293–301.
10. Alsop DC, Detre JA. Multislice perfusion imaging using arterial spin labeling and an amplitude modulated control. Presented at the International Society for Magnetic Resonance in Medicine 1997. Vancouver, BC. April 14, 1997.
11. Siewert B, Schlaug G, Edelman RR, Warach S. Comparison of EPISTAR and T2*-weighted gadolinium-enhanced perfusion imaging in patients with acute cerebral ischemia. Neurology 1997;48:673–679.
12. Powers WJ. Cerebral hemodynamics in ischemic cerebrovascular disease. Ann Neurol 1991;29:231–240.
13. Carpenter DA, Grubb RL Jr, Powers WJ. Borderzone hemodynamics in cerebrovascular disease. Neurology 1990;40:1587–1592.
14. Leblanc R, Yamamoto YL, Tyler JL, Diksic M, Hakim A. Borderzone ischemia. Ann Neurol 1987;22:707–713.
15. Powers WJ, Tempel LW, Grubb RL Jr. Influence of cerebral hemodynamics on stroke risk: one-year follow-up of 30 medically treated patients. Ann Neurol 1989;25:325–330.
16. Nighoghossian N, Trouillas P, Philippon B, Itti R, Adeleine P. Cerebral blood flow reserve assessment in symptomatic versus asymptomatic high-grade internal carotid artery stenosis. Stroke 1994;25:1010–1013.
17. Gur AY, Bova I, Bornstein NM. Is impaired cerebral vasomotor reactivity a predictive factor of stroke in asymptomatic patients? Stroke 1996;27:2188–2190.
18. Bogousslavsky J, Delaloye-Bischof A, Regli F, Delaloye B. Prolonged hypoperfusion and early stroke after transient ischemic attack. Stroke 1990;21:40–46.
19. Webster MW, Makaroun MS, Steed DL, Smith HA, Johnson DW, Yonas H. Compromised cerebral blood flow reactivity is a predictor of stroke in patients with symptomatic carotid artery occlusive disease. J Vasc Surg 1995;21:338–345.
20. Group DTTS. Predictors of major vascular events in patients with a transient ischemic attack or nondisabling stroke. Stroke 1993;24:527–531.
21. Mull M, Schwarz M, Thron A. Cerebral hemispheric low-flow infarcts in arterial occlusive disease; lesion patterns and angiomorphological conditions. Stroke 1997;28:118–123.

22. Pantoni L, Garcia JH, Gutierrez JA. Cerebral white matter is highly vulnerable to ischemia. Stroke 1996;27:1641–1647.
23. Weiller C, Ringelstein E, Reiche W, Buell U. Clinical and hemodynamic aspects of low-flow infarcts. Stroke 1991;22: 1117–1123.
24. Watanabe N, Imai Y, Nagai K, et al. Nocturnal blood pressure and silent cerebrovascular lesions in elderly Japanese. Stroke 1996;27:1319–1327.
25. Dixon WT, Du LN, Faul DD, Gado M, Rossnick S. Projection angiograms of blood labeled by adiabatic fast passage. Magn Reson Med 1986;3:454–462.
26. Alsop DC, Detre JA. Multi-slice cerebral blood flow imaging with continuous arterial spin labeling MRI. Radiology 1998; in press.
27. Alsop DC. Correction of ghost artifacts and distortion in echo-planar MR imaging with an iterative reconstruction technique. Radiology 1995;197P:388. Abstract.
28. Weisskoff RM, Davis TL. Correcting gross distortions in echoplanar images. In: Proceedings of the XI annual meeting of the Society of Magnetic Resonance in Medicine 1992;3:4515. Abstract.
29. Alsop DC, Detre JA. Reduction of excess noise in fMRI time series data using noise image templates. Presented at the International Society for Magnetic Resonance in Medicine 1997. Vancouver, BC. April 16, 1997.
30. Maccotta L, Detre JA, Alsop DC. The efficiency of adiabatic inversion for perfusion imaging by arterial spin labeling. NMR Biomed 1997;10:216–221.
31. Heiss WD, Huber M, Fink GR, et al. Progressive derangement of periinfarct viable tissue in ischemic stroke. J Cereb Blood Flow Metab 1992;12:193–203.
32. Baron JC, Rougemont D, Soussaline F, et al. Local interrelationships of cerebral oxygen consumption and glucose utilization in normal subjects and in ischemic stroke patients: a positron tomography study. J Cereb Blood Flow Metab 1984; 4:140–149.
33. Pekar J, Jezzard P, Roberts DA, Leigh JS J, Frank JA, McLaughlin AC. Perfusion imaging with compensation for asymmetric magnetization transfer effects. Magn Reson Med 1996;35:70–79.
34. Zhang W, Williams DS, Detre JA, Koretsky AP. Measurement of brain perfusion by volume-localized NMR spectroscopy using inversion of arterial water spins: accounting for transit time and cross relaxation. Magn Reson Med 1992;25:362–371.
35. Marchal G, Furlan M, Beaudouin V, et al. Early spontaneous hyperperfusion after stroke. A marker of favorable tissue outcome. Brain 1996;119:409–419.
36. Hakim AM, Pokrupa RP, Villanueva J, et al. The effect of spontaneous reperfusion on metabolic function in early human cerebral infarcts. Ann Neurol 1987;21:279–289.
37. Ueda T, Hatakeyama T, Kumon Y, Sakaki S, Uraoka T. Evaluation of risk of hemorrhagic transformation in local intra-arterial thrombolysis in acute ischemic stroke by initial SPECT. Stroke 1994;25:298–303.
38. Sorensen AG, Buonanno FS, Gonzalez RG, et al. Hyperacute stroke: evaluation with combined multisection diffusion-weighted and hemodynamically weighted echo-planar MR imaging. Radiology 1996;199:391–401.
39. Hossmann KA. Viability thresholds and the penumbra of focal ischemia. Ann Neurol 1994;36:557–565.
40. Astrup J, Siesjo BK, Symon L. Thresholds in cerebral ischemia—the ischemic penumbra. Stroke 1981;12:723–725.
41. Moseley ME, Kucharczyk J, Mintorovitch J, et al. Diffusion-weighted MR imaging of acute stroke: correlation with T2-weighted and magnetic susceptibility-enhanced MR imaging in cats. AJNR Am J Neuroradiol 1990;11:423–429.
42. Warach S, Chien D, Li W, Ronthal M, Edelman RR. Fast magnetic resonance diffusion-weighted imaging of acute human stroke. Neurology 1992;42:1717–1723.
43. Warach S, Gaa J, Siewert B, Wielopolski P, Edelman RR. Acute human stroke studied by whole brain echo planar diffusion-weighted magnetic resonance imaging. Ann Neurol 1995;37:231–241.